

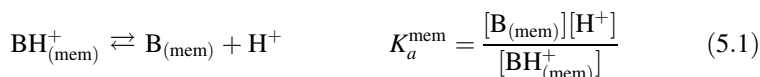
CHAPTER 5

PARTITIONING INTO LIPOSOMES

The octanol–water partition model has several limitations; notably, it is not very “biological.” The alternative use of liposomes (which are vesicles with walls made of a phospholipid bilayer) has become more widespread [149,162,275, 380–444]. Also, liposomes contain the main ingredients found in all biological membranes.

5.1 TETRAD OF EQUILIBRIA AND SURFACE ION PAIRING (SIP)

Figure 5.1 shows a tetrad of equilibrium reactions related to the partitioning of a drug between an aqueous environment and that of the bilayer formed from phospholipids. (Only half of the bilayer is shown in Fig. 5.1.) By now, these reaction types might be quite familiar to the reader. The subscript “mem” designates the partitioning medium to be that of a vesicle formed from a phospholipid bilayer. Equations (4.1)–(4.4) apply. The pK_a^{mem} in Fig. 5.1 refers to the “membrane” pK_a . Its meaning is similar to that of pK_a^{oct} ; when the concentrations of the uncharged and the charged species *in the membrane phase* are equal, the *aqueous* pH at that point defines pK_a^{mem} , which is described for a weak base as



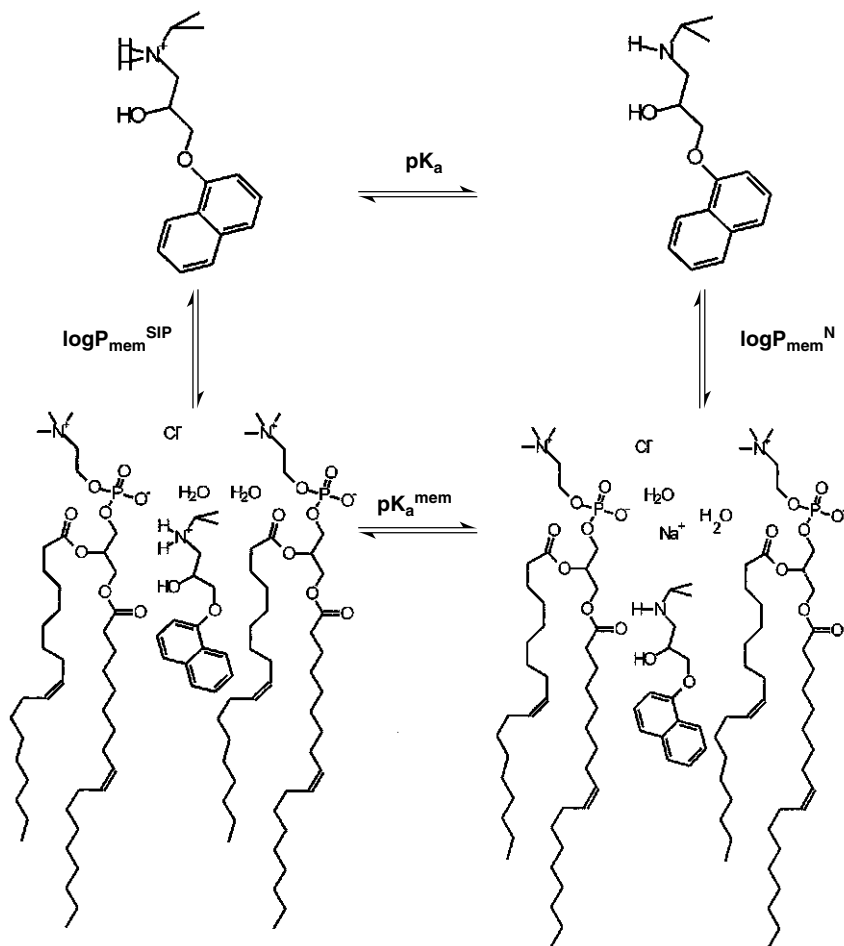


Figure 5.1 Phospholipid membrane–water tetrad equilibria. Only half of a bilayer is shown. [Avdeef, A., *Curr. Topics Med. Chem.*, **1**, 277–351 (2001). Reproduced with permission from Bentham Science Publishers, Ltd.]

The salt dependence of constants discussed in Section 4.2 also applies to the pK_a^{mem} and $\log P_{mem}^{SIP}$ constants. Although they are *conditional*, the dependence on ionic strength is subtle [433,442]. It is thought that when a charged drug migrates into the lipid environment of a liposome, the counterion that at first accompanies it may be exchanged with the zwitterionic phosphatidylcholine head groups, as suggested in Fig. 5.1. As the nature of the ion pair may be different with liposome partitioning, the term *surface ion pair* (SIP) is used to denote it. We use the term $diff_{mem}$ to designate the difference between the neutral species partitioning and the surface ion pair partitioning [see Eq. (4.6)].

5.2 DATABASES

There are no convenient databases for liposome log P values. Most measured quantities need to be ferreted from original publications [149,162,376,381–387,443]. The handbook edited by Cevc [380] is a comprehensive collection of properties of phospholipids, including extensive compilations of structural data from X-ray crystallographic studies. Lipid-type distributions in various biological membranes have been reported [380,388,433].

5.3 LOCATION OF DRUGS PARTITIONED INTO BILAYERS

Based on the observed nuclear Overhauser effect in a $^{31}\text{P}\{^1\text{H}\}$ nuclear magnetic resonance (NMR) study of egg phosphatidylcholine (eggPC) bilayers, Yeagle et al. [399] concluded that the *N*-methyl hydrogens were in close proximity to phosphate oxygens in neighboring phospholipids, suggesting that the surface of the bilayer was a “shell” of interlocking (intermolecular) electrostatic associations. Added cholesterol bound below the polar head groups, and did not interact with them directly. However, its presence indirectly broke up some of the surface structure, making the surface more polar and open to hydration.

Boulanger et al. [420,421] studied the interactions of the local anesthetics procaine and tetracaine with eggPC multilamellar vesicles (MLV, 52–650 mM), as a function of pH, using deuterium nmr as a structural probe. They proposed a three-site model, similar to that in Fig. 5.1, except that the membrane-bound species (both charged and uncharged) had two different locations, one a weakly bound surface site (occupied at pH 5.5), and the other a strongly bound deeper site (occupied at pH 9.5). Membrane partition coefficients were estimated for both sites. Westman et al. [422] further elaborated the model by applying the Gouy–Chapman theory. When a charged drug partitions into the bilayer, a Cl^- is likely bound to the surface, to maintain charge neutrality. They found unexpected low values of diff_{mem} of 0.77 for tetracaine and 1.64 for procaine (see Section 4.7). Kelusky and Smith [423], also using deuterium NMR, proposed that at pH 5.5, there was an electrostatic bond formed between the protonated drug and the phosphate groups, ($\equiv\text{P}-\text{O}^- \cdots ^+\text{H}_3\text{N}-$), and a hydrogen bond formed between the aminobenzene proton and the acyl carbonyl oxygen. At pH 9.5, the ionic bond breaks as the secondary amine moves deeper into the interior of the bilayer; however, the aminobenzene H bond, ($=\text{CO} \cdots \text{H}_2\text{N}-$), continues to be an anchoring point.

Bäuerle and Seelig [395] studied the structural aspects of amlodipine (weak base, primary amine $\text{p}K_a$ 9.26 [162]) and nimodipine (nonionizable) binding to phospholipid bilayers, using NMR, microcalorimetry, and zeta-potential measurements. They were able to see evidence of interactions of amlodipine with the *cis* double bond in the acyl chains. They saw no clear evidence for ($\equiv\text{P}-\text{O}^- \cdots ^+\text{H}_3\text{N}-$) electrostatic interactions.

Herbette and co-workers [425–428,445] studied the structures of drugs bound to liposomes using a low-angle X-ray diffraction technique. Although the structural

details were coarse, it was apparent that different drugs position in different locations of the bilayer. For example, amlodipine is charged when it partitions into a bilayer at physiological pH; the aromatic dihydropyridine ring is buried in the vicinity of the carbonyl groups of the acyl chains, while the $-\text{NH}_3^+$ end points toward the aqueous phase, with the positive charge located near the phosphate negative-charge oxygen atoms [426–428]. A much more lipophilic molecule, amiodarone (weak base with $\text{p}K_a$ 9.1 [$p\text{ION}$]), positioned itself closer to the center of the hydrocarbon interior [425].

5.4 THERMODYNAMICS OF PARTITIONING: ENTROPY- OR ENTHALPY-DRIVEN?

Davis et al. [394] studied the thermodynamics of the partitioning process of substituted phenols and anisoles in octanol, cyclohexane, and dimyristoylphosphatidylcholine (DMPC) at 22°C (which is *below* the gel–liquid transition temperature of DMPC). Table 5.1 shows the results for 4-methylphenol. The phenol partitioned into the lipid phases in the order DMPC > octanol > cyclohexane, as indicated by ΔG_{tr} . Thus, the free energy of transfer into DMPC was greater than into octanol or cyclohexane. Partitioning was generally entropy driven, but the components of the free energy of transfer were greatly different in the three lipid systems (Table 5.1). Octanol was the only lipid to have an exothermic heat of transfer (negative enthalpy), due to H-bond stabilization of the transferred solute, not found in cyclohexane. Although ΔH_{tr} in the DMPC system is a high positive number (endothermic), not favoring partitioning into the lipid phase, the entropy increase (+114.1 eu) was even greater, more than enough to offset the enthalpy destabilization, to end up an entropy-driven process. The large ΔH_{tr} and ΔS_{tr} terms in the DMPC system are due to the disruption of the ordered gel structure, found below the transition temperature.

The partition of lipophilic drugs into lipid phases is often believed to be entropy-driven, a hydrophobic effect. Bäuerle and Seelig [395] studied the thermodynamics of amlodipine and nimodipine binding to phospholipid bilayers (*above* the transition temperature) using highly sensitive microcalorimetry. The partitioning of the drugs into the lipid bilayer was enthalpy-driven, with $\Delta H_{\text{tr}} -38.5 \text{ kJ mol}^{-1}$ bound amlodipine. The entropy of transfer is *negative*, contrary to the usual interpretation

TABLE 5.1 Energy of Transfer (kJ/mol) into Lipid Phase for 4-Methylphenol

Component	DMPC	Octanol	Cyclohexane
ΔH_{tr}	+92.0	-7.3	+18.6
$T\Delta S_{\text{tr}}$	+114.1	+9.2	+22.2
ΔG_{tr}	-22.1	-16.5	-3.6

of the hydrophobic effect. Thomas and Seelig [397] found the partitioning of the Ca^{2+} antagonist, flunarizine (a weak base), also to be predominantly enthalpy-driven, with $\Delta H_{\text{tr}} - 22.1 \text{ kJ mol}^{-1}$, again at odds with the established ideas of entropy-driven partitioning of drugs. The same surprise was found for the partitioning of paclitaxil [398]. These observations thus appear to suggest that drugs partition into membrane phases because they are lipophilic, and not because they are hydrophobic! This needs to be investigated more extensively, using microcalorimetry.

5.5 ELECTROSTATIC AND HYDROGEN BONDING IN A LOW-DIELECTRIC MEDIUM

Section 3.3.4 pointed out that cosolvents alter aqueous ionization constants; as the dielectric constant of the mixture decreases, acids appear to have higher $\text{p}K_a$ values and bases appear (to a lesser extent than acids) to have lower values. A lower dielectric constant implies that the force between charged species increases, according to Coulomb's law. The equilibrium reaction in Eq. (3.1) is shifted to the left in a decreased dielectric medium, which is the same as saying that $\text{p}K_a$ increases. Numerous studies indicate that the dielectric constant in the region of the polar head groups of phospholipids is ~ 32 , the same as the value of methanol. [381,446–453] Table 5.2 summarizes many of the results.

These and other values [381,406] allow us to depict the dielectric spectrum of a bilayer, shown in Fig. 5.2. Given this view, one can think of the phospholipid bilayer as a dielectric *microlamellar* structure; as a solute molecule positions itself closer to the center of the hydrocarbon region, it experiences lower dielectric field (Fig. 5.2). At the very core, the value is near that of vacuum. A diatomic molecule of Na^+Cl^- in vacuum would require more energy to separate into two distinct ions than that required to break a single carbon–carbon bond!

This means that ions will not easily enter the interior of bilayers without first forming contact ion pairs. It is reasonable to imagine that simple drug–counterion pairs, such as $(\text{BH}^+ \cdots \text{Cl}^-)$ will undergo exchange of charge pairs (BH^+ for Na^+ originally in the vicinity of $\equiv\text{PO}^-$) on entering the head-group region, to form, for example, $(\equiv\text{PO}^- \cdots {}^+\text{HB})$, with the release of Na^+ and Cl^- , as depicted in Fig. 5.1. We called such an imagined pairing SIP in Section 5.1 [149].

An interesting hypothesis may be put forward. The interfacial $\text{p}K_a^{\text{mem}}$ (Fig. 5.1) that a solute exhibits depends on the dielectric environment of its location in the bilayer. Simple isotropic water-miscible solvents may be used to approximate $\text{p}K_a^{\text{mem}}$. Pure methanol (ϵ 32), may do well for the bilayer zone containing the phosphate groups; pure 1,4-dioxane (ϵ 2) may mimic some of the dielectric properties of the hydrocarbon region. It appears that $\text{p}_s K_a$ values of several weak bases, when extrapolated to 100% cosolvent, do approximate $\text{p}K_a^{\text{mem}}$ values [119,162,172]. Fernández and Fromherz made favorable comparisons using dioxane [448]. This idea is of considerable practical use, and has been largely neglected in the literature.

TABLE 5.2 Dielectric Constants of Water–Lipid Interfaces (Expanded from Ref. 453)^a

Type	Site	Method	ϵ	Ref.
Unilamellar vesicles (PC, α T) ^a	Polar head/acyl core	Chemical reaction, α T-DPPH	26	446
Unilamellar vesicles PC	Polar head/acyl core	Fluorescence polarization (DSHA)	33	381
Unilamellar vesicles PC+10% cholesterol	Polar head/acyl core	Fluorescence polarization (DSHA)	40	381
Unilamellar vesicles PC+20% stearylamine	Polar head/acyl core	Fluorescence polarization (DSHA)	43	381
Unilamellar vesicles PC+20% cardiolipin	Polar head/acyl core	Fluorescence polarization (DSHA)	52	381
Unilamellar vesicles, PC	Hydrocarbon core	Fluorescence polarization (AS)	2	381
Multilamellar PC	Polar head/bulk water	Fluorescence polarization (ANS)	32	447
Multilamellar PC	Polar head/acyl core	Fluorescence polarization (<i>NnN'</i> -DOC)	25	447
Unilamellar vesicles (PC, DPPC)	Polar head/acyl core	Fluorescence depolarization (DSHA)	32	450
Unilamellar vesicles (PC, α T)	Polar head/acyl core	Chemical reaction, α T-DPPH	29–36	453
GMO bilayers	Polar head/acyl core	Electrical time constant	30–37	451
Micelles (CTAB, SDS, Triton-X100)	Aqueous surface	Fluorescence (HC, AC)	32	448
Micelles (various types)	Aqueous surface	Fluorescence (<i>p</i> -CHO)	35–45	449
Micelles (SDES, SDS, STS)	Aqueous surface	Absorption wavelength maximum	29–33	452

^aAbbreviations: α T = α -tocopherol, AC = aminocoumarin, ANS = 1-anilino-8-naphthalenesulfonic acid, CTAB = cetyltrimethylammonium bromide, DPPC = dipalmitoylphosphatidylcholine, DPPH = 1,1-diphenyl-2-picrylhydrazyl, DSHA = *N*-dansylhexadecylamine, GMO = glycerol monooleate, HC = hydrocoumarin, *N,N'*-DOC = *N,N'*-di(octadecyl)oxacarbocyanine, PC = phosphatidylcholine, *p*-CHO = pyrene carboxaldehyde, SDES = sodium decyl sulfate, SDS = sodium dodecyl sulfate, STS = sodium tetradecyl sulfate.

The molecular view of the interactions of drug molecules with phospholipid bilayers, suggested graphically in Fig. 5.1, has (1) an electrostatic component of binding with the head groups, which depends on the dielectric constant; (2) a hydrogen bonding component, since the phospholipids are loaded with strong H-bond acceptors ready to interact with solutes having strong H-bond donor groups; and (3) a hydrophobic/lipophilic component. Interactions between drugs and bilayers are like that of a solute and a ‘fuzzy, delocalized’ receptor with the microlamellar zones (Fig. 5.2) *electrostatic* ··· *H bond* ··· *hydrophobic*. It is useful to explore this idea, and we will do so below.

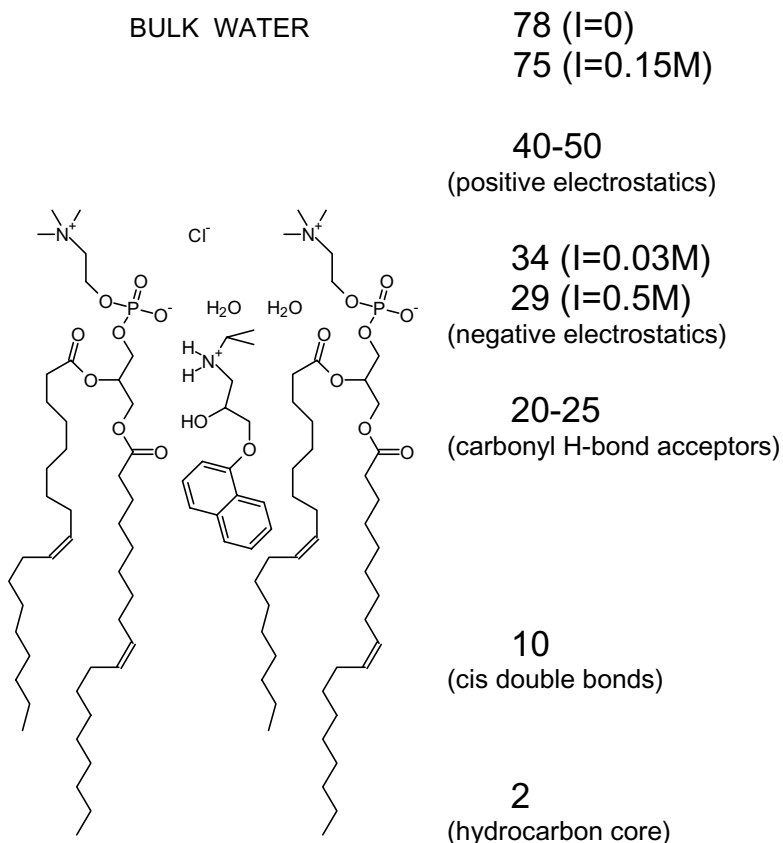


Figure 5.2 Approximate dielectric properties of a phospholipid bilayer, compiled from a number of sources, summarized in Table 5.2. [Avdeef, A., *Curr. Topics Med. Chem.*, **1**, 277–351 (2001). Reproduced with permission from Bentham Science Publishers, Ltd.]

5.6 WATER WIRES, H⁺/OH⁻ CURRENTS, AND THE PERMEABILITY OF AMINO ACIDS AND PEPTIDES

The stability of vesicular pH gradients (between the inner and outer aqueous solutions) depends on processes that can allow protons to permeate across phospholipid barriers. Phospholipid bilayers are thought not to be permeable to charged species (per the pH partition hypothesis). However, some studies suggest H⁺/OH⁻ permeability to be surprisingly high, as high as 10⁻⁴ cm/s, greatly exceeding that of about 10⁻¹² cm/s for Na⁺ [409–419]. Biegel and Gould [409] rapidly changed the pH (acid pulse measurements) of a suspension of small unilamellar vesicles (SUVs; soybean PC) from the equilibrated pH 8.2 to the external pH 6.7, and monitored the rate of influx of H⁺ into the vesicles. (The pH inside of vesicles can be measured by fluorescent probes [409,419].) It took several minutes for the internal

pH to drop from pH 8.2 to 7.4. This time was long because charge transfer led to buildup of a potential difference across the membrane (Donnan potential), which was slow to dissipate. The time was dropped to about 300 ms in the presence of a K^+ ionophore, valinomycin, an antiporter type of effect. The proton ionophore, bis(hexafluoroacetyl)acetone, dropped the reequilibration time down to <1 ms.

Discussions of the possible mechanisms of H^+ transport ensued. It was pointed out that the solubility of water in *n*-alkanes was high enough to suggest the participation of membrane-dissolved water in the transport mechanism. Biegel and Gould [409] predicted that the SUVs used in their study could have 30–40 H_2O molecules dissolved in the bilayer hydrocarbon (HC) core. Meier et al. [411] measured the concentration of water in the HC interior of bilayers to be about 100 mM. Two short reviews discussed proton conductance: Nagle [412] defended the position that “water wires” inside the HC core can explain H^+ conductance; Gutknecht [413] questioned that view, proposing that fatty acid impurities can also explain the phenomenon, in a flip-flop movement of the neutralized weak acid. Proton carriers such as CO_2 or H_2CO_3 could also be involved [415]. The last word has not been said on this topic.

Using liposomes made from phospholipids as models of membrane barriers, Chakrabarti and Deamer [417] characterized the permeabilities of several amino acids and simple ions. Phosphate, sodium and potassium ions displayed effective permeabilities $0.1\text{--}1.0 \times 10^{-12}$ cm/s. Hydrophilic amino acids permeated membranes with coefficients $5.1\text{--}5.7 \times 10^{-12}$ cm/s. More lipophilic amino acids indicated values of $250\text{--}410 \times 10^{-12}$ cm/s. The investigators proposed that the extremely low permeability rates observed for the polar molecules must be controlled by bilayer fluctuations and transient defects, rather than normal partitioning behavior and Born energy barriers. More recently, similar magnitude values of permeabilities were measured for a series of enkephalin peptides [418].

5.7 PREPARATION METHODS: MLV, SUV, FAT, LUV, ET

Working with liposomes requires considerable care, compared to octanol. Handling of liposomes is ideally done under an inert atmosphere at reduced temperatures. Prepared suspensions ought to be stored frozen when not used. Air oxidation of *cis* double bonds is facile; hydrolysis of esters to form free fatty acids (FFAs) is usually a concern. The best commercial sources of phospholipids have $<0.1\%$ FFA. Procedurally, a dry chloroform solution of a phospholipid is placed in a round-bottomed glass flask. Argon is allowed to blow off the chloroform while the flask is vortexed; a thin multilamellar layer forms on the glass surface. After evacuation of the residual chloroform, a buffer is added to the flask, and the lipid is allowed to hydrate under vortexing agitation, with argon gas protecting the lipid from air oxidation. A suspension of multilamellar vesicles (MLVs; diameter >1000 nm) forms in this way. [162] Small unilamellar vesicles (SUV, 50 nm

diameters) can be made by vigorous sonication of MLVs. [385,386] Hope and coworkers developed procedures for preparing large unilamellar vesicles (LUV, 100–200 nm diameter) by an extrusion technique (ET), starting from the MLV suspension [389–391]. Freeze-and-thaw (FAT) steps are needed to distribute buffer salts uniformly between the exterior aqueous solution and the aqueous solution trapped inside vesicles [390]. Methods for determining volumes of liquid trapped inside the vesicles have been discussed [392]. When liposome surfaces are modified by covalent attachment of polyethylene glycol (PEG) polymer, the so-called stealth liposomes can evade the body's immune system, and stay in circulation for a long time, acting like a Trojan horse bearing drugs [393]. Such systems have been used in drug delivery [391,393]. Ordinary liposomes carrying drugs are quickly dismembered by the immune system.

For partition studies, only SUV [385,386] or LUV [149] should be used; MLVs have many layers of trapped solution, which usually cause hysteresis effects [162].

5.8 EXPERIMENTAL METHODS

The determination of partition coefficients using liposomes as a lipid phase require that the sample be equilibrated with a suspension of liposomes, followed by a separation procedure, before the sample is quantitated in the fraction free of the lipid component.

Miller and Yu [444] used an ultrafiltration method to separate the drug-equilibrated liposomes from the aqueous solution, in a study of the effect of cholesterol and phosphatidic acid on $\log P_{\text{mem}}^N$ and $\log P_{\text{mem}}^{\text{SIP}}$ values of pentobarbitone, as a function of pH. Herbetts and colleagues [425–428] and Austin et al., [441,442] and others [433] used ultrafiltration/centrifugation to separate the drug-laden liposomes from the aqueous solution. Wunderli-Allenspach's group [435–438] and others [381,383,384] used equilibrium dialysis for the separation step, the "gold standard" method [311]. It is the gentlest (and slowest) procedure. One reported high-throughput method may speed things up [454]. An interesting new method is based on the use of phospholipid-impregnated porous resin [317,318,376]. Trapped MLVs form in the rehydrated resin. Drug samples are allowed to equilibrate with the suspended particles, and then the solution is simply filtered. The filtrate is assayed for the unbound sample. No separation of phases is required when the NMR method is used [439,440]. Line broadening as a function of pH was used to determine partitioning into liposomes.

The pH-metric method, which also requires no phase separation, has been used to determine drug–liposome partitioning [149,162,385–387]. The method is the same as that described in Section 4.14, except that FAT-LUV-ET liposomes are used in place of octanol. SUV liposomes have also been used [385,386]. To allow for pH gradients to dissipate (Section 5.6) in the course of the titration, at least 5–10 min equilibration times are required between successive pH readings.

5.9 PREDICTION OF $\log P_{\text{mem}}$ FROM $\log P$

In a very comprehensive study, Miyoshi et al. [381] measured $\log P_{\text{mem}}^N$ of 34 substituted phenols using four eggPC liposome systems: (1) lecithin, (2) lecithin + 10 mol% cholesterol, (3) lecithin + 20 mol% cardiolipin (negative charge), and (4) lecithin + 20 mol% stearylamine (positive charge). They probed the dielectric properties of the interfacial and the hydrocarbon core regions of the four systems using *N*-dansylhexadecylamine (DSHA) and anthroylstearic acid (AS) fluorescent probes. Phenol concentrations ranged from 10 to 100 μM ; the unilamellar liposome suspensions, 5 mg/mL, were prepared in a 40 mM aspartate buffer at pH 6. Equilibrium dialysis (12 h) was used for the partition coefficients determination. Fujita's group [381] found that surface polarity increases with charged lipids; interfacial dielectric constants, ϵ (see Table 5.2), were estimated as 33 (unmodified), 40 (cholesterol), 43 (stearylamine), and 52 (cardiolipin). (There was minimal effect in the hydrocarbon core: ϵ 2.1, 1.9, 2.0, 2.0, respectively.) As ϵ increased, the membrane surface becomes more hydrated, with weakened inter-head-group interactions. Cholesterol appears to lead to tighter chain packing, weaker inter-head-group interactions, producing a more hydrated surface (see Section 5.3). The membrane $\log P_{\text{mem}}^N$ values were compared to those of the octanol–water system, $\log P_{\text{oct}}^N$, with the following (quantitative structure–property relation (QSPR)) derived

$$\delta = \log P_{\text{mem}}^N - \log P_{\text{oct}}^N = 0.82 - 0.18 \log P_{\text{oct}}^N + 0.08 \text{HB} - 0.12 \text{VOL} \quad (5.2)$$

where HB refers to H-bond donor strength ($\text{HB} = \text{p}K_a^H - \text{p}K_a^R$, where $\text{p}K_a^H$ is the reference phenol value), and VOL is related to a steric effect. For a substituted phenol with a $\log P_{\text{oct}}^N$ near zero, the $\log P_{\text{mem}}^N$ value is ~ 0.82 . This “membrane advantage” factor is sensitive to ionic strength effects, and may be indicative of an electrostatic interaction. As the octanol $\log P$ value increases, the δ factor decreases from the 0.82 base level, as the negative coefficient -0.18 suggests, which can be interpreted to mean that the membrane is less lipophilic than octanol (more alkane like). The H-bonding coefficient, $+0.08$, indicates that the H-bond acceptor property in membranes is greater than that of octanol, and strong H-bond donor phenols will show higher membrane partitioning, compared to octanol. The last term in Eq. (5.2) indicates that membranes do not tolerate steric hindrance as well as octanol; bulky di-ortho substituents produces higher VOL values.

Figure 5.3 illustrates the key features of the Fujita study. In relation to the reference phenol in frame (a), frames (b), and (c) illustrate the effect of H-bonding, and frames (d) and (e) illustrate steric hindrance. Given that the H-bond donor strength of (b) is greater than that of (c), since $\text{p}K_a$ (b) $<$ $\text{p}K_a$ (c), the relative membrane partitioning, δ , increases in (b) and decreases in (c), relative to (a). Similarly, steric hindrance in (d) produces negative δ , compared to (e).

A plot of δ versus $\log P_{\text{oct}}^N$ of 55 substituted phenols, combining the data from Fujita's group [381] with those of Escher et al. [382,383] is shown in Fig. 5.4. The slope-intercept parameters listed in the figure are close to the values in Eq. (5.2).

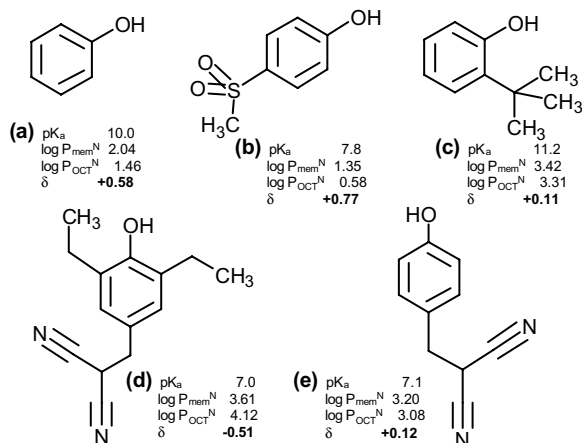


Figure 5.3 The effect of hydrogen bonding and steric hindrance on the difference between liposome–water and octanol–water partition coefficients δ ; increased H-bond donor strength and decreased steric hindrance favor membrane partitioning in the substituted phenols [381]. [Avdeef, A., *Curr. Topics Med. Chem.*, **1**, 277–351 (2001). Reproduced with permission from Bentham Science Publishers, Ltd.]

The homologous series of (*p*-methylbenzyl)alkylamines [387] indicates an interesting $\delta/\log P_{\text{Oct}}^N$ plot, shown in Fig. 5.5. The slope factor of the smaller members of the series, -1.02 , is larger than that of the phenol series. The value being near 1 indicates that $\log P_{\text{mem}}^N$ is invariant with the octanol partition constant—the

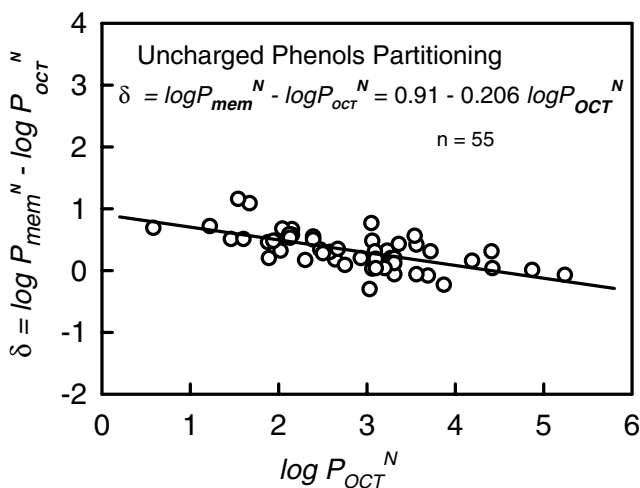


Figure 5.4 Comparing liposome–water to octanol–water partition coefficients of a series of uncharged substituted phenols [381–383]. [Avdeef, A., *Curr. Topics Med. Chem.*, **1**, 277–351 (2001). Reproduced with permission from Bentham Science Publishers, Ltd.]

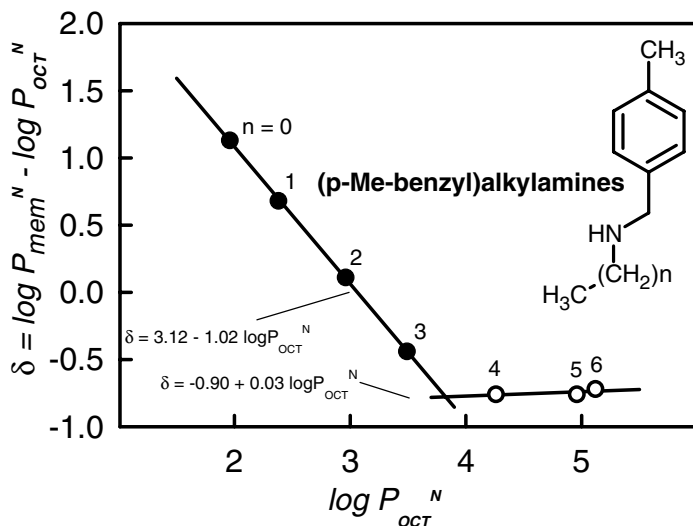


Figure 5.5 Comparing liposome–water to octanol–water partition coefficients of a series of uncharged substituted benzylalkylamines [387]. The membrane partitioning of the smaller members of the series ($n = 0 \dots 3$) is thought to be dominated by electrostatic and H-bonding effects (enthalpy-driven), whereas the partitioning of the larger members is thought to be directed by hydrophobic forces (entropy-driven) [387]. [Avdeef, A., *Curr. Topics Med. Chem.*, **1**, 277–351 (2001). Reproduced with permission from Bentham Science Publishers, Ltd.]

membrane partitioning does not change for $n = 0$ – 3 in the series. For $n = 4$ – 6 the octanol and membrane partition coefficients change at about the same rate. For longer-chain members of the series, the partitioning in both solvent systems expresses hydrophobicity (entropy-driven). However, for the short-chain members, various electrostatic and polar interactions play a role, and partitioning in the membrane system is not sensitive to the length of the chain (enthalpy-driven). It would be illuminating to subject this series to a precision microcalorimetric investigation.

When unrelated compounds are examined [149,162,385,386,429], exclusive of the phenols and the amines just considered, the variance of the relationship is considerably higher, but the general trend is evident, as seen in Fig. 5.6; the higher the octanol–water partition coefficient, the smaller is the δ difference between membrane and octanol partitioning. The slope of the relationship in Fig. 5.6 is about twice that found for phenols. For molecules with $\log P^N_{\text{oct}}$ between 2 and 4, δ values are close to zero, indicating that the partition coefficients for many drug molecules are about the same in octanol as in phospholipid bilayers [149]. However, outside this interval, the differences can be substantial, as the next examples show. For *hydrophilic* molecules, the membrane partition coefficient is surprisingly high, in comparison to that of octanol. For example, acyclovir has $\log P^N = -1.8$ in octanol–water but $+1.7$ in liposome–water, indicating a δ of $+3.5$ log units. Similar trends are found for other hydrophilic molecules, such as famotidine or zidovudine (Fig. 5.6). Atenolol and xamoterol also have notably high $\log P^N_{\text{mem}}$ values [433].

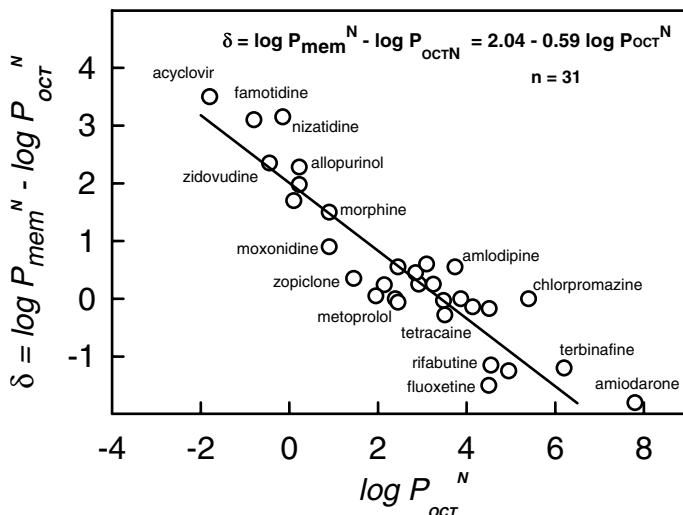


Figure 5.6 The difference between liposome–water and octanol–water partitioning as a function of the octanol–water partition coefficient for a series of unrelated structures [149,385,386,429]. For example, acyclovir partitions into liposomes over 3000 times more strongly than into octanol, and amiodarone partitions into liposomes 100 times more weakly than into octanol. [Avdeef, A., *Curr. Topics Med. Chem.*, **1**, 277–351 (2001). Reproduced with permission from Bentham Science Publishers, Ltd.]

At the opposite extreme is the example of amiodarone. The log octanol partition coefficient is 7.8 [162], whereas the membrane constant is reported as 6.0 [429], surprisingly, almost two orders of magnitude smaller ($\delta = -1.8$).

Although the relationship in Fig. 5.6 is somewhat coarse, it is still useful in predictions. Since octanol–water $\log P$ prediction programs are omnipresent and adequately reliable, it can now be said that they can predict membrane–water partitioning, by using the equation in Fig. 5.6. Better yet, if one measures the value of $\log P_{\text{oct}}^N$, one can estimate the membrane partition coefficient with the confidence of the variance expressed in Fig. 5.6.

5.10 $\log D_{\text{mem}}$, diff_{mem} , AND THE PREDICTION OF $\log P_{\text{mem}}^{\text{SIP}}$ FROM $\log P^I$

In the preceding section, we explored the relationship between $\log P_{\text{oct}}^N$ and $\log P_{\text{mem}}^N$. We now focus on the partitioning of the charged species into phospholipid bilayer phases. More surprises are in store.

Figure 5.7 shows lipophilicity profiles ($\log D$ vs. pH) for an acid (warfarin), a base (tetracaine), and an ampholyte (morphine). The dashed curves correspond to the values determined in octanol–water and the solid curves, to values in liposome–water. As is readily apparent, the major differences between octanol and liposomes

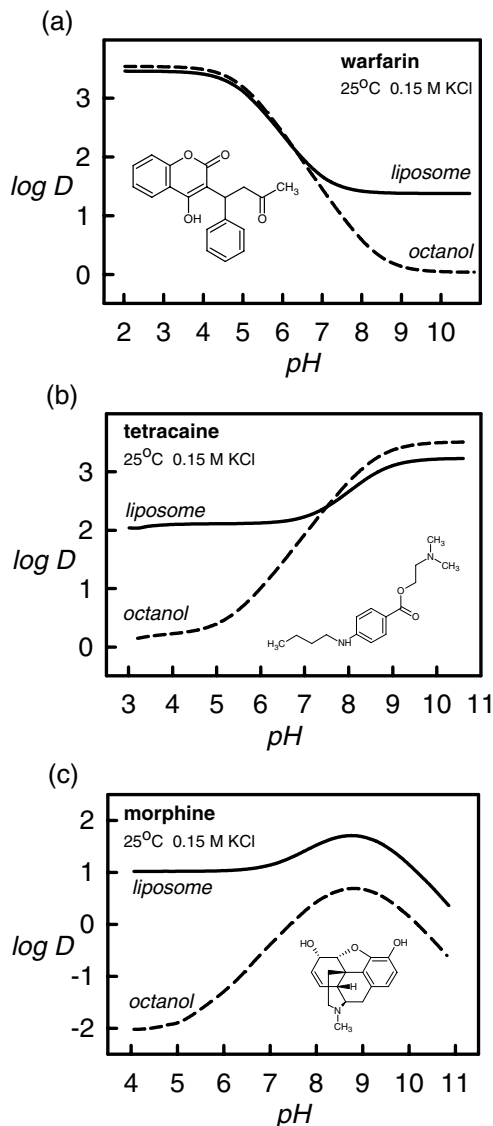


Figure 5.7 Comparison of liposome–water (solid lines) to octanol–water (dashed lines) lipophilicity profiles for a weak acid, a weak base, and an ampholyte. [Avdeef, A., *Curr. Topics Med. Chem.*, **1**, 277–351 (2001). Reproduced with permission from Bentham Science Publishers, Ltd.]

occur in the pH regions where charged-species partitioning takes place. In Section 4.7 we noted that octanol–water $\text{diff}(\log P^{N-1})$ values for simple acids were ~ 4 and for simple bases ~ 3 . When it comes to liposome–water partitioning, the “diff 3–4” rule appears to slip to the “diff 1–2” rule. This is evident in Figs. 5.7a,b. The smaller diff_{mem} values in membrane systems have been noted

for some time, for example, with reported $\text{diff}_{\text{mem}} = 0$ for tetracaine, 1 for procaine and lidocaine [455], and $\text{diff}_{\text{mem}} = 1.45$ for tetracaine [424]. Miyazaki et al. [396] considered diff_{mem} values of 2.2 for acids and 0.9 for bases in their study of dimyristoylphosphatidylcholine (DMPC) bilayer dispersions. Other studies indicated similar diff values [149,383–386,433–438,441,442]. It seems that charged species partition into membranes about 100 times more strongly than suggested by octanol.

Alcorn et al. [433] studied the partitioning of proxicromil (acid: $\text{p}K_a$ 1.93, log $P_{\text{oct}}^N \sim 5$, log P_{oct}^I 1.8 [456]) in MLV liposomes prepared from reconstituted brush-border lipids (slightly negatively charged at pH 7.4). Membrane partition coefficients were determined by the centrifugation (15 min, 150 kg) method. It was observed that in 0.15 M NaCl background, proxicromil showed a nearly constant log D_{mem} (3.0–3.5) at pH 4–9, which was unexpected, given the $\text{p}K_a$. However, when the background salt was lowered to 0.015 M, the expected curve shape (log D_{mem} 3.5 at pH 3 and 1.5 at pH 9) was observed, similar to that in Fig. 5.7a. Interestingly, the researchers took the solutions at pH 8 and titrated them with NaCl and LiCl. The log D_{mem} seen in the 0.15 M NaCl medium was reestablished by titration (more easily with NaCl than LiCl). The ionic strength dependence can be explained by the Gouy–Chapman theory [406,407]. The sample concentration (1.67 mM) was high enough to cause a buildup of negative charge on the surface. Without the high 0.15 M NaCl to shield the surface charge, sample anion-anion electrostatic repulsion on the membrane surface prevented the complete partitioning of the drug, making it appear that log D_{mem} was lowered. The Na^+ titration reduced the surface charge, allowing more anionic drug to partition. The fact that the Na^+ titrant is more effective than the Li^+ titrant can be explained by the higher hydration energy of Li^+ , making it less effective at interacting with the membrane surface [400]. Incidentally, we predict the log P_{mem}^N of proxicromil using the relationship in Fig. 5.6 to be ~ 4 , in very acceptable agreement with the observed value.

In well-designed experiments, Pauletti and Wunderli-Allenspach [435] studied the partitioning behavior of propranolol in eggPC at 37°C, and reported log D_{mem} for pH 2–12. SUVs were prepared by the controlled detergent method. The equilibrium dialysis method was used to determine the partition coefficients, with propranolol concentration (10^{-6} to 10^{-9} M) determined by liquid scintillation counting. The lipid concentration was 5.2 mM. Internal pH of liposomes was checked by the fluorescein isothiocyanate method. Gradients in pH were dissipated within 5 min after small pH changes in the bulk solution. The lipophilicity curve they obtained is very similar in shape to that of tetracaine, shown in Fig. 5.7b. The log $P_{\text{mem}}^N = 3.28$ and log $P_{\text{mem}}^{\text{SIP}} = 2.76$ values indicate $\text{diff}_{\text{mem}} = 0.52$.

Austin et al. [441] reported the partitioning behavior of amlodipine, 5-phenylvaleric acid, 4-phenylbutylamine, and 5-hydroxyquinoline at 37°C in 1–100 mg mL⁻¹ DMPC SUVs. The ultrafiltration (10 kDa cutoff) with mild (1.5 kg) centrifugation method was used to determine partition coefficients. Sample concentrations were $3\text{--}8 \times 10^{-5}$ M. Most remarkably, $\text{diff}_{\text{mem}} = 0.0$ was observed for amlodipine. A similarly low value of 0.29 was reported for 4-phenylbutylamine. Furthermore, the partitioning behavior was unchanged by ionic strength changes in the interval 0.0–0.15 M, seemingly in contradiction to the effect observed by Alcorn and co-workers. They proposed that charged molecules associated with the charged head

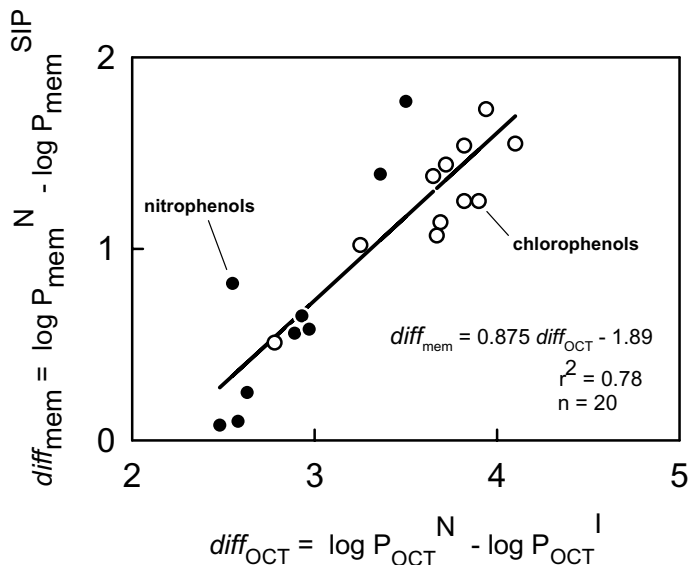


Figure 5.8 Comparison of liposome *diff* to octanol *diff* functions of substituted phenols [382,383]. [Avdeef, A., *Curr. Topics Med. Chem.*, **1**, 277–351 (2001). Reproduced with permission from Bentham Science Publishers, Ltd.]

groups of the phospholipids, an effect they preferred not to call “ion pairing.” Undeniably, the nature of the charged-species partitioning into phospholipid bilayers is different from that found in octanol.

In a later study, Austin et al. [442] effectively were able to reconcile the ionic strength differences between their study and that of Alcorn et al. [433], using a Gouy–Chapman model. When the drug concentration in the membrane is plotted against the drug concentration in water, the resultant hyperbolic curve shows a lessening slope ($\log D$) with increasing drug concentration (10^{-6} to 10^{-4} M) when there is no background salt. This is consistent with the interpretation that surface-bound charged drug repulsion attenuates additional charged drug partitioning. Bäuerle and Seelig [395] and Thomas and Seelig [397] observed hyperbolic curves with drug concentrations exceeding $1 \mu\text{M}$. The addition of 0.15 M NaCl mitigates the effect substantially, allowing for higher drug concentrations to be used.

Avdeef et al. [149] and Balon et al. [385,386] reported $\log P_{\text{mem}}^N$ and $\log P_{\text{mem}}^{\text{SIP}}$ values of a number of drugs, determined by the pH-metric method, using both LUVs and SUVs, in a background of 0.15 M KCl.

Escher and colleagues [383,384] reported SIP values for a large series of substituted phenols, using DOPC SUVs and the equilibrium dialysis/centrifugation method. Figure 5.8 is a plot of diff_{mem} versus diff_{oct} for the series of phenols studied by Escher. It appears that knowing the octanol *diff* values can be useful in predicting the membrane values, and for phenols the relationship is described by

$$\text{diff}_{\text{mem}} = 0.88 \text{diff}_{\text{oct}} - 1.89 \quad (5.3)$$

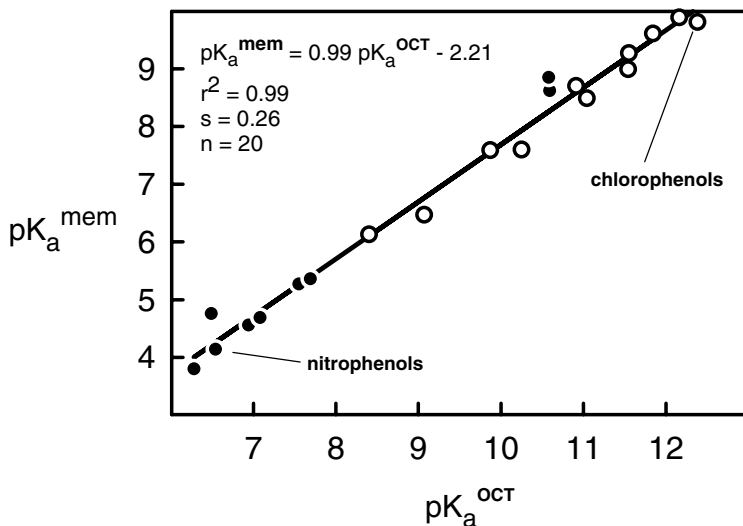


Figure 5.9 The remarkable relationship between the octanol and the membrane pK_a values of a series of substituted phenols [382,383]. [Avdeef, A., *Curr. Topics Med. Chem.*, **1**, 277–351 (2001). Reproduced with permission from Bentham Science Publishers, Ltd.]

The offset of 1.89 indicates that surface ion pairing in membranes is about 100 times greater than that of octanol. Scherrer suggested that comparisons of pK_a^{OCT} to pK_a^{mem} may be more predictive [276]. Indeed, this is true for the phenols, as indicated in Fig. 5.9. It is remarkable that the relation for the phenols

$$pK_a^{\text{mem}} = 0.99 pK_a^{\text{OCT}} - 2.21 \quad (5.4)$$

has an r^2 of 0.99, for 20 compounds. Again, we see the 2.21 offset, indicating that the 100-fold slippage from the *diff* 3-4 rule to the *diff* 1-2 rule. This harbors good prediction relations.

The well-behaved prediction of charged phenol partitioning is less certain when carried over to unrelated structures, as shown in Fig. 5.10, for the molecules reported by Avdeef et al. [149] and Balon et al. [385,386].

5.11 THREE INDICES OF LIPOPHILICITY: LIPOSOMES, IAM, AND OCTANOL

Taillardat-Bertschinger et al. [311] explored the molecular factors influencing retention of drugs on IAM columns, compared to partitioning in liposomes and octanol. Twenty-five molecules from two congeneric series (β -blockers and (*p*-methylbenzyl)alkylamines; see Fig. 5.5) and a set of structurally unrelated drugs were used. Liposome-buffer partitioning was determined by the equilibrium dialysis and the pH-metric methods. The intermethod agreement was good, with r^2 0.87.

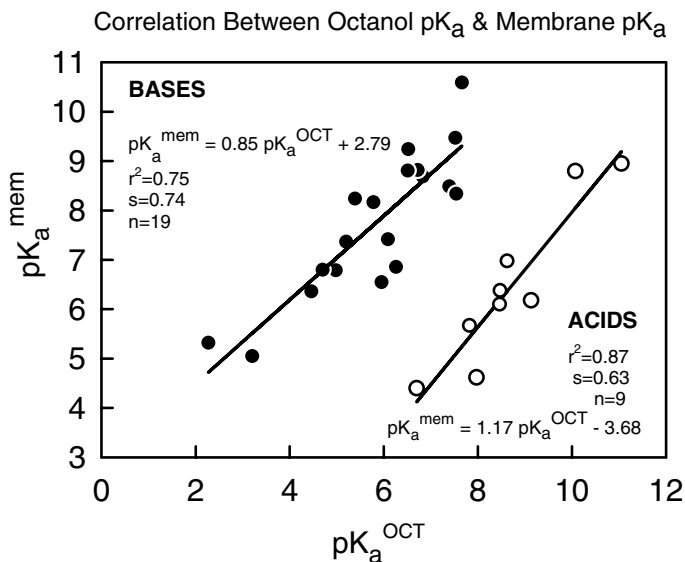


Figure 5.10 Comparison of membrane to octanol pK_a values of compounds with unrelated structures [149,385,386]. [Avdeef, A., *Curr. Topics Med. Chem.*, **1**, 277–351 (2001). Reproduced with permission from Bentham Science Publishers, Ltd.]

However, when the IAM $\log k_{IAMw}^{7.0}$ were compared to liposome $\log D_{\text{mem},7.0}$, there was no direct correlation when all of the compounds were used. It was clear that multi-mechanisms were operative, in the Lipinski sense [1].

For the series of large molecules, such as, β blockers or the long-chain (*p*-methylbenzyl)alkylamines, IAM retention correlated with liposome partitioning. Hydrophobic recognition forces was thought to be responsible for the partitioning process. In addition, the formation of an H bond between the hydroxy group of the β blocker and the ester bond of phospholipids (Fig. 5.1) may explain why the β blockers partitioned into the liposomes more strongly than the alkylamines. For the more hydrophilic short-chain (*p*-methylbenzyl)alkylamines ($n = 0-3$ in Fig. 5.5), the balance between electrostatic and hydrophilic interactions was different in the IAM and liposome systems. Electrostatic interactions are thought to play only a minor role for the IAM retention of the model solutes, presumably due to the smaller density of phospholipids in IAM resin surfaces, compared to liposomes. The solute's capacity to form H-bonds, which is important for partitioning in liposomes, plays only a minor role in the IAM system.

5.12 GETTING IT WRONG FROM ONE-POINT $\log D_{\text{mem}}$ MEASUREMENT

In the early literature, it was a common practice to make a single measurement of $\log D$, usually at pH 7.4, and use a simplified version of Eq. (4.10) (with $\log P^I$

neglected) along with the known pK_a to calculate $\log P^N$. (The practice may still persist today. We have intentionally omitted these simplified equations in this book.) Most of the time this produced the correct $\log P^N$, often because ion pairing was not extensive at the pH of measurement. This is true for the β blockers whose pK_a is about 9.5; the *diff* 3–4 rule would suggest that ion pair partitioning should be extensive only below pH 6.5.

With liposome partitioning, however, the rule slips to *diff* 1–2. This means SIP partitioning starts at about pH 8.5 for weak bases whose pK_a values are near 9.5 (e.g., Figs. 5.7b, 5.11). So, all who published “anomalous” values of $\log P_{\text{mem}}^N$ may need to get out their slide rules [429–432]! (What we know now was not known then.)

5.13 PARTITIONING INTO CHARGED LIPOSOMES

Wunderli-Allenspach’s group reported several partition studies where drugs interacted with liposomes that were charged [368,436–438]. Although not entirely surprising, it was quite remarkable that propranolol partitions into negatively charged liposomes with $\log P_{\text{mem}}^N$ 3.49 and $\log P_{\text{mem}}^{\text{SIP}}$ 4.24 [438], compared to values determined with neutral liposome values $\log P_{\text{mem}}^N$ 3.27 and $\log P_{\text{mem}}^{\text{SIP}}$ 2.76 [435]. Negatively charged liposomes can enhance the surface ion pair (SIP) partitioning of positively charged propranolol by a factor of 30. The unusually-shaped lipophilicity profile is shown in Fig. 5.11, for the system where negative charge is imparted by 24 mol% oleic acid in the eggPC.

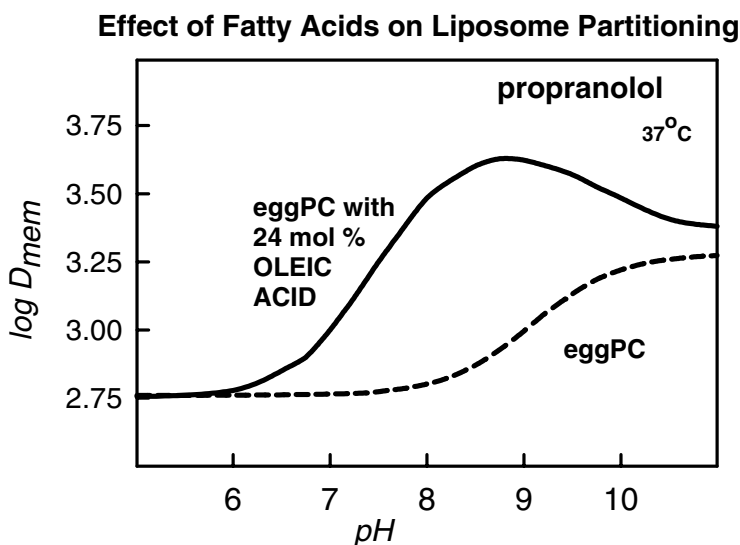


Figure 5.11 Lipophilicity profiles of propranolol in liposome–water (dashed curve) and liposome–water, where the liposome phase had 24 mol% FFA, imparting a negative charge to the surface above pH 6 [436]. [Avdeef, A., *Curr. Topics Med. Chem.*, **1**, 277–351 (2001). Reproduced with permission from Bentham Science Publishers, Ltd.]

Since the FFA is an anion $>pH$ 7 and propranolol a cation $<pH$ 9, there is a window of opportunity between pH 7 and 9 for electrostatic attraction of propranolol into the membrane phase, as indicated in Fig. 5.11. Note how similar the curve shapes in Fig. 5.11 are to some of the curves in Fig. 4.6b.

5.14 pK_a^{mem} SHIFTS IN CHARGED LIPOSOMES AND MICELLES

Ionizable molecules embedded in the surfaces of lipids, such as octanol (see Fig. 2.8), liposomes (see Fig. 5.2), or micelles, will have their apparent pK_a values shifted. With *neutral* lipids, the pK_a of an acid increases and the pK_a of a base decreases. This is due to the effect of the decreased dielectric constant in the interfacial zone, as we have already discussed in various sections.

An additional (electrostatic) shift occurs if the lipid vesicles or micelles have a charged surface, according to the expression suitable for monoprotic acids and bases

$$pK_a^{mem} = pK_a \pm diff_{mem} - \frac{F\phi}{2.3RT} \quad (5.5)$$

where the terms have their usual meanings, with \pm being $+$ sign for acids, $-$ sign for bases [396,404,406, 407,448,457,458]. At $25^\circ C$ and using mV (millivolt) units to express the surface potential, ϕ , the rightmost term in eq. 5.5 becomes $\phi/59.16$. The rationale for the electrostatic term goes like this: if the surface is negatively charged, then it will attract protons into the interfacial zone, such that the interfacial pH will be lower than the bulk pH , by the amount of $|\phi/59.16|$. A proton fog envelops the negatively charged vesicle. Since the proton concentration is in the pK_a expression [Eq. (3.1)], the apparent pK_a changes accordingly.

Consider negatively charged liposomes made from a mixture of phosphatidylcholine (PC) and phosphatidylserine (PS). Unlike the zwitterionic head group of PC (invariant charge state, $pH > 3$), the head group of PS has two ionizable functions for $pH > 3$: the amine and the carboxylic acid. In physiologically neutral solution, the PS group imparts a negative charge to the liposome (from the phosphate). Titrations of PS-containing liposomes reveal the pK_a values of 5.5 for the carboxylic acid group and 11.5 for the amine group [403]. When the head-group molecule itself (free of the acyl HC chains), phosphoserine (Fig. 5.12), is titrated, the observed pK_a values for the two sites are 2.13 and 9.75, respectively [162].

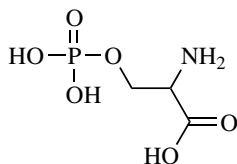


Figure 5.12 Phosphoserine.

According to the *diff* 1–2 rule, we should have expected to see the pK_a 4.13 (carboxylate) and 8.75 (amine), but the liposome titration shows something else. Instead, we have an “anomalous” additional shift of +1.37 for the carboxylic group and a +2.75 for the amine group. These extra shifts are due to the negatively charged surface of the liposomes! We can estimate, using Eq. (5.5), that when the carboxylic group is titrated in the PS liposome, the surface charge is -81 mV (pH 5.5), and when the amine group is titrated, the surface charge drops to -163 mV (pH 11.5). Conversely, if we had a way of estimating surface charge,

TABLE 5.3 Critically Selected Experimental Liposome–Water Partition Coefficients

Compound	$\log P_{\text{mem}}^N$	$\log P_{\text{mem}}^{\text{SIP}}$	t^a (°C)	Ref.
4-Phenylbutylamine	2.39	2.48	—	149
5-Phenylvaleric acid	3.17	1.66	—	149
Acetylsalicylic acid	2.40	1.60	37	385
Acyclovir	1.70	2.00	37	385
Allopurinol	2.50	2.70	37	385
Amiloride	1.80	1.60	37	385
Amlodipine	4.29	4.29	—	— ^b
Atenolol	2.20	1.00	37	385
Carvedilol	4.00	4.20	—	— ^b
Chlorpromazine	5.40	4.45	—	— ^b
Diclofenac	4.34	2.66	—	149
Famotidine	2.30	1.70	37	385
Fluoxetine	3.00	2.20	37	385
Furosemide	3.00	1.90	37	385
Ibuprofen	3.87	1.94	—	149
Lidocaine	2.39	1.22	—	149
Metoprolol	2.00	1.25	37	385
Miconazole	3.70	2.90	37	385
Morphine	1.89	1.02	—	— ^b
Moxonidine	1.80	1.30	—	385
Nizatidine	3.00	2.80	37	385
Olanzapine	3.70	2.70	37	385
Paromomycin	1.70	1.20	37	385
Procaine	2.38	0.76	—	149
Propranolol	3.45	2.61	—	149
Rifabutine	3.40	3.50	37	385
Terbinafine	5.00	3.00	37	385
Tetracaine	3.23	2.11	—	149
Warfarin	3.46	1.38	—	149
Xipamide	3.30	1.70	37	385
Zidovudine	1.90	2.40	37	385
Zopiclone	1.80	1.40	37	385

^aTemperature 25°C, unless otherwise stated.

^bSirius Analytical Instrument Ltd.

TABLE 5.4 Liposome–Water Partition Coefficients of Substituted Phenols and Other Compounds

Compound	$\log P_{\text{mem}}^N$	$\log P_{\text{mem}}^{\text{SIP}}$	Note/Ref.
Phenol	1.97	—	— ^a
2-Cl-phenol	2.78	1.57	— ^{a,b}
3-Cl-phenol	2.78	—	— ^a
4-Cl-phenol	2.92	2.43	— ^{a,b}
2,4-Di-Cl-phenol	3.54	2.41	— ^{a,b}
2,6-Di-Cl-phenol	2.83	1.09	— ^{a,b}
3,4-Di-Cl-phenol	3.82	2.82	— ^b
2,4,5-Tri-Cl-phenol	4.35	2.80	— ^b
2,4,6-Tri-Cl-phenol	3.82	2.59	— ^{a,b}
3,4,5-Tri-Cl-phenol	4.72	3.18	— ^b
2,3,4,5-Tetra-Cl-phenol	4.88	3.63	— ^b
2,3,4,6-Tetra-Cl-phenol	4.46	3.39	— ^b
penta-Cl-phenol	5.17	3.79	— ^b
2-NO ₂ -phenol	2.09	0.70	— ^b
4-NO ₂ -phenol	2.72	0.95	— ^b
2,4-Di-NO ₂ -phenol	2.73	1.94	— ^{a,b}
2,6-Di-NO ₂ -phenol	1.94	1.84	— ^b
2-Me-4,6-di-NO ₂ -phenol	2.69	2.46	— ^{a,b}
4-Me-2,6-di-NO ₂ -phenol	2.34	2.26	— ^b
2- <i>s</i> -Bu-4,6-di-NO ₂ -phenol	3.74	3.33	— ^{a,b}
2- <i>t</i> -Bu-4,6-di-NO ₂ -phenol	4.10	3.54	— ^b
4- <i>t</i> -Bu-2,6-di-NO ₂ -phenol	3.79	3.21	— ^b
2-Me-phenol	2.45	—	— ^a
3-Me-phenol	2.34	—	— ^a
4-Me-phenol	2.42	—	— ^a
2-Et-phenol	2.81	—	— ^a
4-Et-phenol	2.88	—	— ^a
2-Pr-phenol	3.13	—	— ^a
4-Pr-phenol	3.09	—	— ^a
2- <i>s</i> -Bu-phenol	3.47	—	— ^a
4- <i>s</i> -Bu-phenol	3.43	—	— ^a
2- <i>t</i> -Bu-phenol	3.51	—	— ^a
3- <i>t</i> -Bu-phenol	3.25	—	— ^a
4- <i>t</i> -Bu-phenol	3.43	—	— ^a
2-Ph-phenol	3.40	—	— ^a
4-Ph-phenol	3.24	—	— ^a
4- <i>t</i> -Pent-phenol	3.64	—	— ^a
2,6-di-Me-phenol	2.47	—	— ^a
2,6-di-Et-phenol	2.73	—	— ^a
3-Me-4-Cl-phenol	3.29	—	— ^a
4-SO ₂ Me-phenol	1.27	—	— ^a
4-CN-phenol	2.11	—	— ^a
4-CF ₃ -phenol	3.25	—	— ^a
3-NO ₂ -phenol	2.56	—	— ^a

TABLE 5.4 (Continued)

Compound	$\log P_{\text{mem}}^N$	$\log P_{\text{mem}}^{\text{SIP}}$	Note/Ref.
2-Et-4,6-di-NO ₂ -phenol	3.02	—	— ^a
2- <i>i</i> -Pr-4,6-di-NO ₂ -phenol	3.14	—	— ^a
Benzenesulphonamide	0.82	—	— ^c
Aniline	1.04	—	— ^c
Nitrobenzene	1.71	—	— ^c
Naphthylamide	1.99	—	— ^c
4-Cl-1-naphthol	2.88	—	— ^c
Naphthalene	2.78	—	— ^c
2-Me-anthracene	3.75	—	— ^c
1,2,5,6-Dibenzanthracene	3.09	—	— ^c
Benzamide	0.21	—	— ^c
Methylphenylsulphone	0.88	—	— ^c
Hydrochlorothiazide	0.91	—	— ^c
Methylphenylsulphoxide	0.98	—	— ^c
Phenylurea	1.04	—	— ^c
Phenylbenzamide	1.05	—	— ^c
Phenol	1.32	—	— ^c
Dimethylphenylsulfonamide	1.60	—	— ^c
Acetophenone	1.76	—	— ^c
Benzonitrile	1.81	—	— ^c
Benzaldehyde	1.90	—	— ^c
Methylnaphthylsulphone	1.91	—	— ^c
Naphthylsulphonamide	2.01	—	— ^c
Anisole	2.10	—	— ^c
Methylbenzoate	2.20	—	— ^c
Triphenylphosphineoxide	2.21	—	— ^c
3-(2-Naphthoxy)propylmethylsulphoxide	2.60	—	— ^c
Chrysene	2.60	—	— ^c
Fluoroanthrene	2.61	—	— ^c
Toluene	2.71	—	— ^c
Phenanthrene	2.75	—	— ^c
Atenolol	—	1.36	— ^c
Xamoterol	—	1.46	— ^c
Proxichromil	—	1.50	— ^{c,d}
Amlodipine	3.75	3.75	— ^e
5-Phenylvaleric acid	2.95	0.50	— ^e
4-Phenylbutylamine	2.41	2.12	— ^e
5-Hydroxyquinoline	1.85	—	— ^e

^aTemperature 25°C, equilibrium dialysis, small unilamellar vesicles (lecithin) [381].

^bTemperature 20°C, equilibrium dialysis, small unilamellar vesicles (DOPC), 0.1 M KCl [382].

^cCentrifugation method (15 min, 150,000 g), brush-border membrane vesicles [433].

^dIonic strength 0.015 M (NaCl).

^eTemperature 37°C, 0.02 M ionic strength, ultrafiltration method, small unilamellar vesicles (DMPC) [441].

say, by zeta-potential measurements [395,397,398], then we could predict what pK_a^{mem} should be. This is an important consideration, since membranes often bear (negative) surface charge.

5.15 PREDICTION OF ABSORPTION FROM LIPOSOME PARTITION STUDIES?

It is clear that charged species partition more strongly into liposomes than anticipated from octanol properties (Figs. 5.7 and 5.11). Although octanol has been a useful model system, it cannot address the role of ionic forces evident in biological membranes. In addition, it is apparent that certain hydrophilic species such as acyclovir, famotidine, atenolol, and morphine partition into liposomes as neutral species more strongly than suggested by octanol measurements (Fig. 2.6). Hydrogen bonding is certain to be a part of this. If amphiphilic charged or H-bonding species have such a strong affinity for membranes, can passive absorption of charged species be facilitated? What does it mean that acyclovir indicates a $\log P_{\text{mem}}$ that is 3.5 units higher than $\log P_{\text{oct}}$? These questions are revisited at the end of the book.

5.16 $\log P_{\text{mem}}^N$, $\log P_{\text{mem}}^{\text{SIP}}$ “GOLD STANDARD” FOR DRUG MOLECULES

Table 5.3 lists a carefully selected collection of $\log P_{\text{mem}}^N$ and $\log P_{\text{mem}}^{\text{SIP}}$ values of drug molecules taken from various literature and some unpublished sources. Table 5.4 contains a similar collection of values for a series of substituted phenols and a variety of mostly uncharged compounds.